International Journal of Theoretical & Applied Sciences, **1**(1): 111-119(2009)

Development of error contour maps for finite element analysis of prestressed concrete beams considering effects of friction

Pushpa Kotwal, K.K. Pathak[1] and S.S. Pagey[2]
Malwa Institute of Technology, Indore
[1]Scientist, Regional Research Laboratory, CSIR, Bhopal
[2]Professor (Retd.), Dept. of Mathematics, Inst. for Excellence in Higher Education, Bhopal

ABSTRACT

Prestressed concrete is one of the most important construction materials. It is being used in all sots of small to big structures like, railway sleepers, buildings, nuclear reactors, bridges etc. In prestressed concrete high tensile strength steel bars are used which are called tendon or prestressing cable. Friction between the cable and the duct causes loss of prestressing force which will affect stress distribution. For analysis purpose cable are modeled by parabola but this approach has two major problems. To overcome these, in this study prestressing cable is modeled by B-spline curve. In a computer based analysis, error is caused due to various sources like input data, truncation or rounding-off. To minimize errors high precision are employed in computing. But it comes on the cost of high computational time. It has been observed, there exist sets of input parameters for which errors are irrespective of precision. In this paper Finite Element Analysis (FEA) of one and five span prestressed concrete beams are carried out considering single and double precision. Effects of Young's modulus and Poisson's ratio are studied in terms of errors in stresses and deflections and effect of friction has been accounted. Guidelines are suggested to select input parameters for minimum errors for single precision Finite Element Analysis.

Keywords: Precision, truncation error, round-off error, finite element analysis, prestressed concrete, friction

INTRODUCTION

Computer uses binary digits to represent numbers and process them by using certain algorithms. In any numerical analysis such as finite element analysis, accuracy of results depends upon the number of significant digits considered for calculation. Whenever the difference of almost equal numbers occur in a calculation significant digits are lost and incorrect digits, which arise due to rounding off errors, are carried in further calculation. Loss of significant digits may be partially avoided by using double precision numbers. Rajasekaran S.(1986), Balaguruswamy E. (1988), Aggarwal S.K. (1986),William S. Dorn and Daniel D. McCracken (1972), Rajaraman V. (1981), Ralph G. Stanton (1985), Steven C. Chapra et. al. (1985), Gourdin A. et. al. (1996), Antia H. M. (1995), John H. Mathews (1994), John R. Rice (1983), Richard W. Hamming (1971) explain the effect of precision on the results. Suvarna Fadnavis (1998) conclude that increase in round-off error of finite precision computation increases exponentially in iterative computations and enters the mainstream computation within 50-60 iterations. According to Thomas Richard McCalla (1967), these may be due to such causes as errors in observation, measurement, recording, transmission, conversion, mathematical model used and in processing. Sushan Kumar (2006) reported effect of round off error in numerical computation. Yoshida et al (1991), Pearse O'Grady et al (1991) discussed errors due to truncation and floating point. Miquel Grau et al (2006) reported the effect of precision on Euler-Chebyshev iterative method.

In finite element analysis a chain of arithmetic operation take place. A very small initial error may accumulate in big one at the end. Numerical error significantly depends on the sensitivities of the input parameters.
In prestressed concrete there is friction between the prestressing tendons and the inside of ducts during tensioning. In this study, effect of friction and precision with respect to Poisson's ratio and Young's modulus is discussed in terms of errors in stresses and deflections for different span prestressed concrete beams.

Finite Element Modeling

Modeling of the prestressing cable for the finite element analysis of a prestressed concrete structure is a tedious process. To represent realistic profile, cable is modeled by B-spline. The cable is considered to be embedded in the concrete and there exists perfect bond between them. For finite element modeling cable is modeled by 3 node bar element and concrete by 9 node plane stress elements (Fig. 1). The shape functions of 3-node curved bar element is given by-

$$N_{c1} = \frac{(\rho - 1)\rho}{2}$$
$$N_{c2} = (1 - \rho)(1 + \rho)$$
$$N_{c3} = \frac{(1 + \rho)\rho}{2} \qquad \text{...(1)}$$

The global co-ordinates inside the curved bar element can be defined by-

$$\overline{X} = \begin{Bmatrix} x \\ y \end{Bmatrix} = \sum_{i=1}^{3} \begin{Bmatrix} x \\ y \end{Bmatrix} N_{ci} = \sum_{i=1}^{3} X_i N_{ci} \qquad \text{...(2)}$$

The tangent vector along ρ axis for the cable is calculated using-

$$\overline{T} = \sum_{i=1}^{3} X_i \frac{dN_{ci}}{d\rho} \qquad \text{...(3)}$$

And the normal vector can be given by-

$$\overline{N} = \frac{1}{\left|\overline{T}\right|^2}\left[\frac{d^2X}{d\rho^2} - \frac{a}{\left|\overline{T}\right|^2}\cdot\frac{dX}{d\rho}\right] \qquad \text{...(4)}$$

Where $a = \dfrac{dX}{d\rho} \bullet \dfrac{d^2X}{d\rho^2}$

The unit tangent and normal vectors can be given by –

$$\bar{t} = \frac{\overline{T}}{\left|\overline{T}\right|} \quad \text{and} \quad \bar{n} = \frac{\overline{N}}{\left|\overline{N}\right|} \qquad \textbf{...(5)}$$

The curvature at any point on the curve can be obtained by (Piskunov,1981) –

$$K = \frac{\left|\dfrac{dX}{d\rho} \times \dfrac{d^2X}{d\rho^2}\right|}{\left\{\left|\dfrac{dX}{d\rho}\right|^2\right\}^{3/2}} \qquad \text{...(6)}$$

Numerator of (Eq.6) is a cross product. The radius of curvature R is given by

$$R = \frac{1}{K} \qquad \text{...(7)}$$

Friction Loss

The cable tension reduces along the length of cable due to friction between the cable and duct. The bar element is assumed to have two Gauss points GP1 & GP2 (fig. 3). The radius of curvature R, obtained above is eq.7 is utilized in the calculation of friction loss. Assume curvature between 1&2 and 2&3 (fig. 2) equal to the curvature R1 & R2. Let the length of the cable between 1-2 and 2-3 be approximated as-

$$L_{1\text{-}2} \approx \sqrt{(x_1 - x_2)^2 + (y_1 - y_2)^2}$$
$$L_{2\text{-}3} \approx \sqrt{(x_2 - x_3)^2 + (y_2 - y_3)^2} \qquad \text{...8)}$$

The tension variation in the bar element can be expressed by isoparametric interpolation as-

$$T_n = \sum_{i=1}^{3} T_i N_{ci} \qquad \text{...(9)}$$

If the radius of curvature at GP1 and GP2 be R_1 and R_2 then tension at 2 & 3 after friction loss will be-

$$T_2 = T_1 e^{(-\mu\alpha_1 - KL_{1-2})}$$
$$T_3 = T_2 e^{(-\mu\alpha_2 - KL_{2-3})} \quad \ldots(10)$$

Where,T_1 = Tension at jacking end for first element. For subsequent elements T_1 will become T_3 of previous element.

$\alpha_1 = L_{1-2} / R_1$
$\alpha_2 = L_{2-3} / R_2$
μ = Coefficient of friction
K = wobble coefficient

In this way cable tension at different locations along cable profile can be obtained.

Forces on concrete due to cable

The cable exerts normal and tangential forces on the concrete due to curvature and friction. These are expressed as-

$$P_t = \frac{dT_n}{dX} = \frac{1}{|\bar{T}|}\frac{dT_n}{d\rho} \quad \ldots(11)$$

$$P_n = \frac{T_n}{R} \quad \ldots(12)$$

Where T_n is the tension in the cable and T is the tangent vector.

The resultant of these is given by –

$$\bar{P} = P_t\bar{t} + P_n\bar{n} \quad \ldots(13)$$

Where $\bar{t}$ and $\bar{n}$ are unit tangent and normal vectors (eq.5).

These loads can be transferred to concrete nodes, using the principle of virtual work. The equivalent nodal force vector for concrete element is expressed as-

$$\{P_L\} = \int_{-1}^{1}[N]^T\{\bar{P}\}|\bar{T}|d\rho \quad \ldots(14)$$

At end elements where cable is anchoraged, cable reaction acts as concentrated loads on the concrete. The anchorage end point forces can be transferred at the nodes in the ratio of shape function and are given by-

$$\{P_A\} = [N]^T\{T_{end}\} \quad \ldots(15)$$

Where, T_{end} is the cable tension at the end points. [N] In Eq.14&15 are the shape functions of nine-node element.

In calculation of Eq.15, local co-ordinates of the anchorage points are required for known global co-ordinates. This is calculated by Newton Raphson iterative method. So, total load vector due to cable concrete interaction is obtained by-

$$\{P\} = \{P_L\} + \{P_A\} \quad \ldots(16)$$

This nodal load vector is applied on the structure along with live and dead load vectors to include prestressing effects.

Computation of Local Co-ordinates (ξ,η)

In above calculation local co-ordinates of known global co-ordinates are required. It is an inverse non-linear problem, which is solved iteratively by Newton-Raphson method as follows. Let (x, y) is the global co-ordinate and (ξ,η) be corresponding local co-ordinate then-

$$\begin{pmatrix}\xi\\ \eta\end{pmatrix}_{i+1} = \begin{pmatrix}\xi\\ \eta\end{pmatrix}_i - \begin{bmatrix}\partial x/\partial\xi & \partial x/\partial\eta\\ \partial y/\partial\xi & \partial y/\partial\eta\end{bmatrix}^{-1}\begin{pmatrix}x_{i+1}-x_i\\ y_{i+1}-y_i\end{pmatrix} \quad \ldots(17)$$

in above equation inverse matrix is nothing but Jacobian matrix. (x_{i+1},y_{i+1}) is the computed value and (x_i, y_i) are the known value. Initial values of (ξ,η) are taken as zero. The computation is carried out iteratively till the difference of two consecutive value of (ξ,η) becomes less than tolerance value. In this study this is taken as 0.001.

Stiffness Matrix

It is assumed that after pre-stressing, the cable is grouted and it becomes integral part of the concrete. The stiffness matrix K is calculated as standard formulation (Zienkiwicz 1991, Chandrapatla 2004)-

$$K = \iiint B^T DBdv \quad \ldots(18)$$

For nine node element, in local (ξ, η) co-ordinate, it becomes-

$$[K] = \int_{-1}^{1}\int_{-1}^{1} B^T DB \det|J| t d\xi d\eta \quad \ldots(19)$$

Where B is element strain displacement matrix, D is material matrix, J is jacobian and t is thickness of the object.

Final load displacement matrix is written as

$$[K]\{U\} = \{P\} \quad \ldots (20)$$

Based on above formulation, finite element software in FORTRAN language, named PRCON2D is developed.

Error in Finite Element Computation

In finite element analysis, while solving the equation KU=P, it is important to note that the elements of the matrices and the computational results can be represented to only a fixed number of digits based on precision, which introduces errors in the solution.

Consider, that in a specific analysis the solution obtained to the equations KU=P is $\overline{U}$; i.e., because of truncation and round off errors, $\overline{U}$ is calculated instead of U. it appears that the error in the solution can be obtained by evaluating a residual ΔP, where

$$\Delta P = P - K\overline{U} \quad \ldots(21)$$

In practice, ΔP would be calculated using double precision arithmetic. Substituting KU for P into (eq.21), we get

$$r = U - \overline{U} \quad \ldots(22)$$

$$r = K^{-1}\Delta P \quad \ldots(23)$$

Although ΔP may be small, the error in the solution may still be large. On the other hand, for an accurate solution ΔP must be small. Therefore a small residual ΔP is a necessary but not a sufficient condition for an accurate solution.

In the solution of KU = P, owing to truncation and round off errors, we may assume that we in fact solve

$$(K + \delta K)(U + \delta U) = P \quad \ldots(24)$$

Assuming that $\delta K \delta U$ is small in relation to other terms, we have approximately

$$\delta U = -K^{-1}\delta K U \quad \ldots(25)$$

Or taking norms,

$$\frac{\|\delta U\|}{\|U\|} \le cond(K)\frac{\|\delta K\|}{\|K\|} \quad \ldots(26)$$

Where cond(K) is the condition number of K,

$$cond(K) = \frac{\lambda_n}{\lambda_1} \quad \ldots(27)$$

Therefore, a large condition number means that solution errors are more likely. To evaluate an estimate of the solution errors, assume that for a t-digit precision computer,

$$\frac{\|\delta K\|}{\|K\|} = 10^{-t} \quad ...(28)$$

Also, assuming s-digit precision in the solution, we have

$$\frac{\|\delta U\|}{\|U\|} = 10^{-s} \quad \ldots(29)$$

Substituting (28) and (29) into (26), we obtain as an estimate of the number of accurate digits obtained in the solution,

$$s \ge t - \log_{10}[cond(K)] \quad \ldots(30)$$

Numerical Examples

Two numerical examples are analyzed to study the effect of input parameters considering single and double precision, on the errors. Effect of friction is also studied. Following material property are taken into account-

(i) Young's modulus = 2×10^4, 3×10^4, 4×10^4, 5×10^4, 6×10^4, 7×10^4 N/mm^2
(ii) Poisson's ratio = 0.00, 0.10, 0.20, 0.30, 0.40
(iii) Wobble coefficient = 1×10^{-5}
(iv) Coefficient of friction = 0.2

(i) Single Span Beam

A single span prestressed concrete beam of 12m length and 100×200 mm cross section is shown in fig. 4. The beam is descretised into 30 elements and 183 nodes. 2 KN prestressing force and 500N point load at center are applied to the beam.

Stress and deflection are calculated by single and double precision computations for different Poisson's ratio and young's modulus. Maximum percent errors in stress and deflection for a set of Poisson's ratio and young's modulus are given in table 1. Based on these maximum errors contour maps are shown in fig. 5 and 6.

It is observed that in case of double precision, stresses are stable and independent of Poisson's ratio and Young's modulus. Corners of contour map at extreme Young's modulus and Poisson's ratio have minimum errors in stress. This error is again minimum for high Young's modulus and is independent of Poisson's ratio.

Small patches of maximum and minimum errors are observed in the contour domain of stress and deflection and these patches are observed for young's modulus 5×10^4 N/mm^2 and Poisson's ratio 0.10 to 0.40. Maximum errors in stress and deflection are concentrated for 2×10^4 N/mm^2 value of Young's modulus and 0.20 value of Poisson's ratio.

(iv) Five Span Beam:

Five span prestressed concrete beam of 250×500 mm cross section is shown in fig. 7. Length of each span of this beam is 8m. The beam is descretised into 40 elements and 243 nodes. 500KN prestressing force and point loads of 50 KN and 100 KN are applied at alternate mid spans of the beam. Reduced prestressing force due to friction at the other end is 193 KN.

Stress and deflection are calculated by single and double precision computations for different Poisson's ratio and young's modulus. Maximum percent errors in stress and deflection for a set of Poisson's ratio and young's modulus are given in table 2. Based on these maximum errors contour maps are shown in fig 8 and 9 .

It is observe that stresses for single and double precision are almost same. Errors in stress are minimum for low Poisson's ratio and 4×10^4 N/mm^2 value of Young's modulus and for Young's modulus = 6×10^4 N/mm^2 and Poisson's ratio = 0.30 also.

Errors in stresses are observed maximum for low Poisson's ratio and high Young's modulus and also for Young's modulus = 6×10^4 N/mm^2 and Poisson's ratio = 0.10. Small patch of maximum errors in deflection is observed at Young's modulus 3×10^4 N/mm^2 .

CONCLUSION

In this study error contour maps for stress and deflection are generated using FE analysis of one and five span beams. Based on these maps, different input parameters for finite element analysis using single precision computation can be selected for minimum error. This will save computational time considerably, especially for large size structure.

REFERENCES

[1] E. Balaguruswamy, Computer oriented statistical and numerical methods. Macmillan India limited, pp 16-20(1988).

[2] D.F. Rogers and J.A. Adams, Mathematical elements for computer graphics, second edition, McGraw Hill, New York. (1990).

[3] A. Gourdin and M. Boumahrat, Applied numerical methods, Prentice Hall India, New Delhi, pp 2-42(1996).

[4] M.K. Hurst, Prestressed concrete design, E & FN SPON, 2nd edition. (1998).

[5] J.H. Mathews, Numerical methods for mathematics, science and engineering", Prentice Hall India, New Delhi, 2nd edition(1994).

[6] J.R. Rice Numerical methods, software and analysis, McGraw Hill, pp 33-56(1983).

[7] Klaus Jürgen Bathe, Finite element procedures, Prentice hall India, New Delhi, pp 734-741(1997).

[8] Klaus Jürgen Bathe, Finite element procedures in engineering analysis, Prentice hall India, New Delhi, pp 481-489(1990).

[9] M.E. Mortenson, Mathematics for Computer Graphics Applications, Industrial Press, New York. (1999).

[10] Pearse O' Grady and Baek-kyu, Young IEEE transactions on computers, **40**(2): (1991).

[11] N Piskunov, Differential and integral calculus part-I, Mir Publishers Moscow. (1989).

[12] D.V. Philips and O.C. Zeinkiewicz, Finite element non-linear analysis of concrete structures , *Proc. Inst. Civil Engrs, Part 2*, **61**: 59-88(1976).

[13] V. Rajaraman, Computer programming in Fortran IV, Prentice Hall of India, New Delhi. (1981).

[14] S. Rajasekaran, Numerical methods in science and engineering – a practical approach, a.h. Wheeler & co. private limited, pp 1-14(1986).

[15] Richard W. Hamming Introduction to applied numerical analysis, McGraw Hill. (1971).

[16] Stanton, Ralph G. Numerical methods for science and engineering, Prentice hall of India New Delhi, pp 109-110(1985).

[17] Steven C. Chapra and Raymond P. Canale Numerical methods for engineers with personal computer application, McGraw Hill, pp 58-90(1985).

[18] Sushan Konar, A divine surprise: The golden mean and round-off error, *Resonance: Journal of science education*, **11**(4): (2006).

[19] Suvarna Fadnavis. Some numerical experiments on round off error growth in finite precision – numerical computation, Xiv: physics/9807003 v1. (1998).

[20] Thomas Richard McCalla, Introduction to numerical methods and FORTRAN programming, John Willey New York, pp 59-70(1967).

[21] William S. Dorn and Daniel D. McCracken, Numerical methods with Fortran IV case studies, John Willy and sons, pp 65-94,(1972).

Table1. Error Analysis for one span beam

Poisson's Ratio	Young's modulus(N/mm^2)	Max. %error for stress	Max. %error for deflection
0.00	2×10^4	14.69	17.39
	3×10^4	9.00	9.81
	4×10^4	130.72	166.77
	5×10^4	4.26	0.63
	6×10^4	2.0833	1.007
	7×10^4	3.79	5.86
0.10	2×10^4	10.38	9.24
	3×10^4	142.92	199.37
	4×10^4	3.7735	4.0268
	5×10^4	16.51	16.35
	6×10^4	113.54	128.46
	7×10^4	24.53	20.82
0.20	2×10^4	408.96	250.42
	3×10^4	4.72	9.81
	4×10^4	52.08	57.71
	5×10^4	26.42	38.78
	6×10^4	2.6041	5.0377
	7×10^4	54.72	64.52
0.30	2×10^4	110.79	196.64
	3×10^4	110.79	145.28
	4×10^4	180.30	220.78
	5×10^4	19.72	10.69
	6×10^4	20.83	22.41
	7×10^4	30.05	37.54
0.40	2×10^4	19.25	21.01
	3×10^4	2.1243	1.3381
	4×10^4	28.64	31.71
	5×10^4	235.21	287.84
	6×10^4	31.09	35.64
	7×10^4	11.26	9.97

Table: 2 Error Analysis for five span beam:

Poisson's Ratio	Young's modulus(N/mm^2)	Max. %error for stress	Max. %error for deflection
0.10	2×10^4	7.6923	1.8867
	3×10^4	7.1428	1.8867
	4×10^4	0.8333	1.005
	5×10^4	7.1428	0.4807
	6×10^4	7.6923	0.1883
	7×10^4	14.28	4.1758
0.20	2×10^4	6.25	0.0000
	3×10^4	10.5231	4.6092
	4×10^4	1.0752	0.8021
	5×10^4	5.8823	0.7042
	6×10^4	5.5555	2.2044
	7×10^4	10.52	4.2056
0.30	2×10^4	5.00	1.0309
	3×10^4	4.1666	0.4219
	4×10^4	4.1666	1.4492
	5×10^4	4.1666	4.83
	6×10^4	8.3333	6.6523
	7×10^4	1.0309	2.506

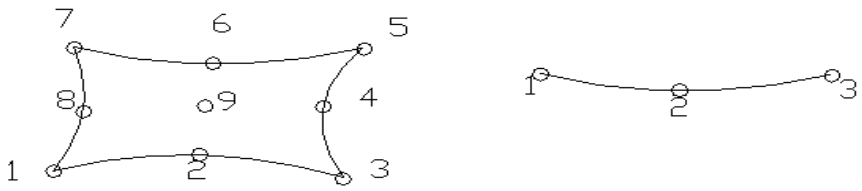

Fig.1. 9-node Langerangian element and 3-node curved bar element

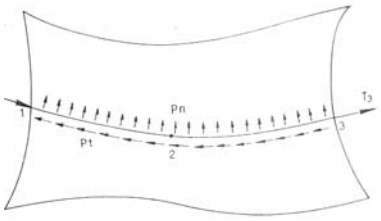

Fig. 2. Force transfer from cable to concrete

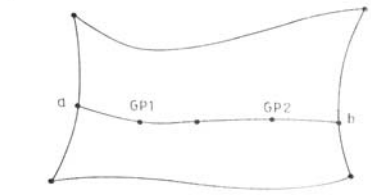

Fig. 3. Curved bar element embedded in concrete

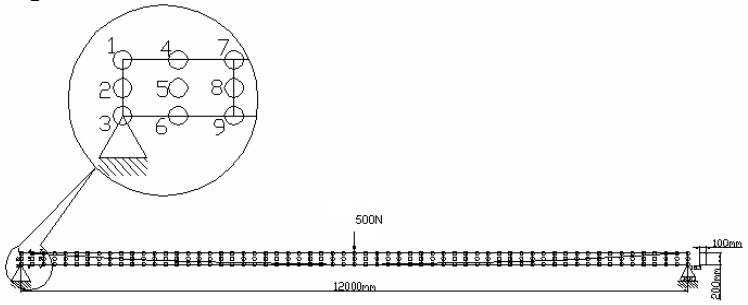

Fig.4. One span beam

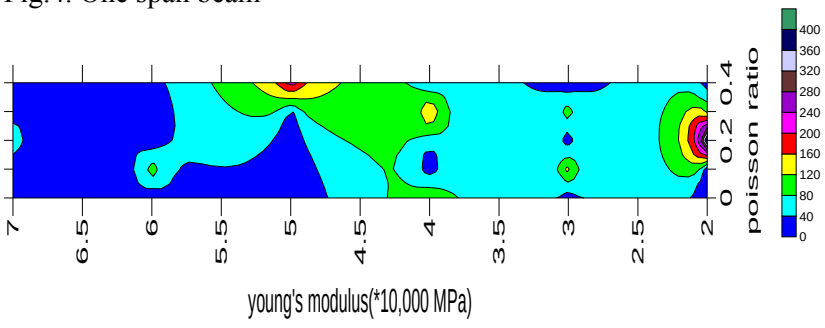

Fig.5. Contour map showing % error in stresses for one span beam

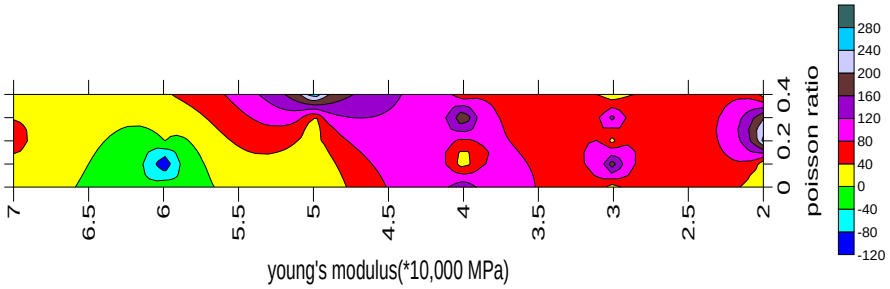

Fig.6. Contour map showing % error in deflection for one span beam

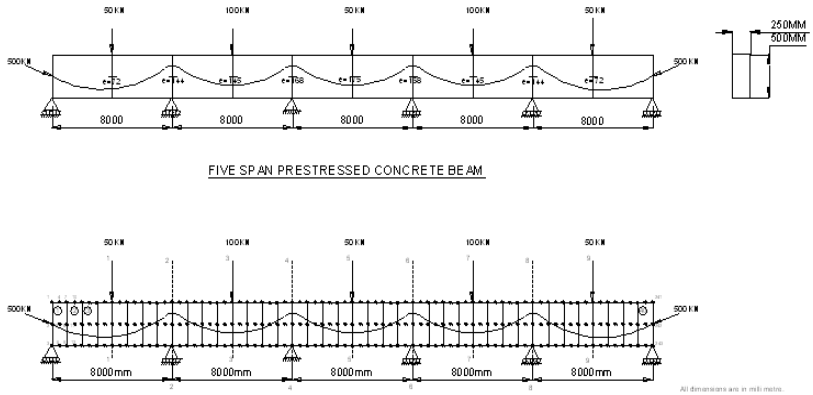

Fig. 7. Discretization and node numbering of five span beam

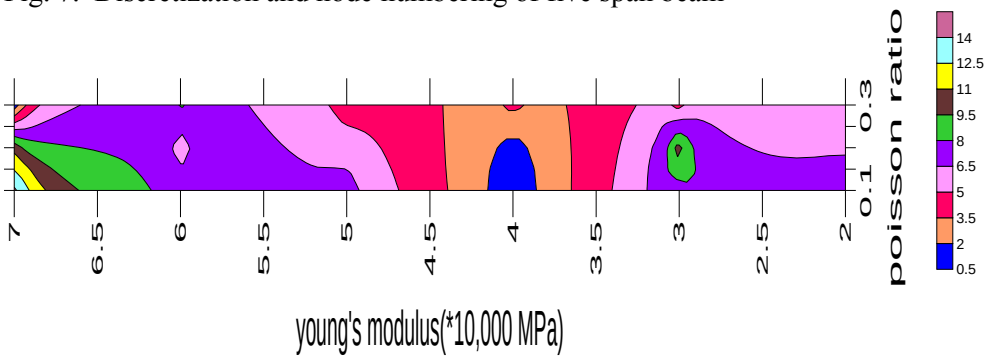

Fig.8. Contour map showing % error in stresses for five span beam

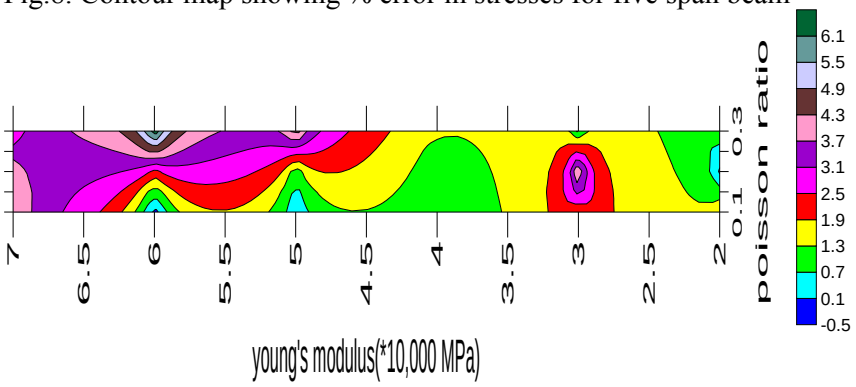

Fig.9. Contour map showing % error in deflections for five span beam